

# Molecular Relaxation Mechanisms of Tyrosine-Derived Polycarbonates by Thermally Stimulated Depolarization Currents

N. SUÁREZ,<sup>1</sup> E. LAREDO,<sup>1</sup> A. BELLO,<sup>1</sup> J. KOHN<sup>2</sup>

<sup>1</sup>Physics Department, Universidad Simón Bolívar, Caracas, Venezuela

<sup>2</sup>Department of Chemistry, Rutgers, The State University of New Jersey, New Brunswick, New Jersey 08903

Received 12 January 1996; accepted 13 June 1996

**ABSTRACT:** A series of tyrosine-derived polycarbonates with different lengths ( $2 \leq n \leq 8$ ) for the alkyl ester pendent chain were studied by measuring thermally stimulated depolarization currents (TSDC). The observed spectra could be separated into three regions: the low-temperature zone with a broad, complex  $\beta$  band (80–240 K), the intermediate zone (250–300 K), and the high-temperature zone (300–400 K) with a sharp  $\alpha$  peak. The application of direct signal analysis (DSA) to decompose the complex peaks into elementary processes led to the determination of the relaxation time distribution and temperature dependence of each process. The variation of the relaxation parameters as a function of the pendent chain length facilitated the tentative identification of the relaxation mechanisms responsible for the observed current peaks. It is proposed that as the temperature increases one observes, first, the individual motion of each polar group, then the concerted motion of the entire pendent chain, and, last, the movement of the polymer backbone. © 1997 John Wiley & Sons, Inc. *J Appl Polym Sci* **63**: 1457–1466, 1997

**Key words:** polycarbonates; tyrosine; dielectric relaxations; TSDC; glass transition; biomaterial

## INTRODUCTION

Tyrosine-derived polycarbonates are new degradable polymers being investigated for medical applications such as drug delivery and bone fixation.<sup>1–4</sup> These degradable polymers represent a specific example of pseudo-poly(amino acid)s and, in this case, are derived from the polymerization of desaminotyrosyl–tyrosine alkyl esters re-

sulting in carbonate–amide copolymers possessing an ester-linked pendent chain (Fig. 1). Previous studies have confirmed that these materials are generally biocompatible, possess favorable physicomaterial properties, and can be fabricated readily into devices useful for medical applications.<sup>5,6</sup>

Currently, the family of tyrosine-derived polycarbonates comprises four polymers whose chemical structure is identical except for the length of an alkyl ester pendent chain present at each monomeric repeat unit. By using the ethyl, butyl, hexyl, or octyl esters, the length of the pendent chains was varied in steps of two methylene groups from two to eight carbons (Fig. 1). The availability of such a series of structurally related polymers facilitated the identification of struc-

---

Correspondence to: J. Kohn

Contract grant sponsor: Consejo Nacional de Investigaciones Científicas y Tecnológicas (CONICIT), Caracas, Venezuela

Contract grant sponsor: Programa de Nuevas Tecnologías

Contract grant number: NM-012

Contract grant sponsor: National Institutes of Health

Contract grant number: GM39455

© 1997 John Wiley & Sons, Inc. CCC 0021-8995/97/111457-10

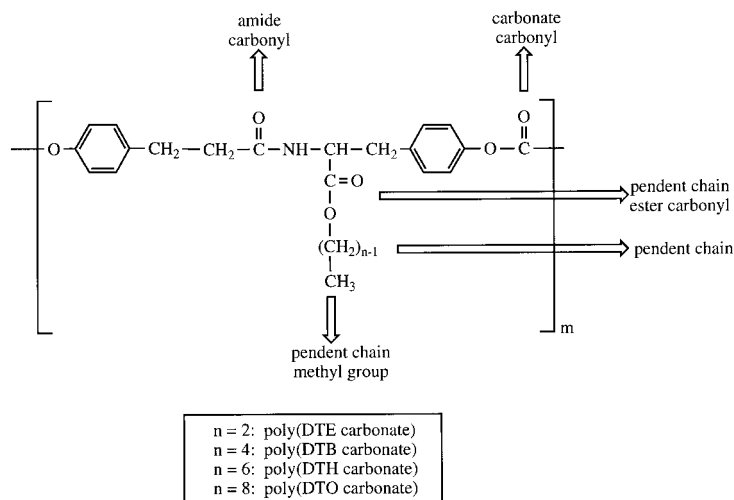


**Figure 1** Chemical structure of polycarbonates derived from desaminotyrosyl-tyrosine alkyl esters. The abbreviations DTE, DTB, DTH, and DTO stand for desaminotyrosyl-tyrosine ethyl ester, desaminotyrosyl-tyrosine butyl ester, desaminotyrosyl-tyrosine hexyl ester, and desaminotyrosyl-tyrosine octyl ester, respectively. Arrows indicate the position of structural units whose motion was observed by TSDC.

ture–property correlations and provided a means to control important material properties. For example, the glass transition temperatures ( $T_g$ ) of this family of polymers decreases in a fairly linear manner from 366 to 325 K as the length of the pendent chain increases.<sup>6</sup>

In a previous study, this same series of four tyrosine-derived polycarbonates was used to study the effect of the length of the pendent chain on the rate of enthalpy relaxation (physical aging).<sup>7</sup> No correlation between the enthalpy relaxation process and the length of the pendent chain was found. This observation suggested that structural relaxation in these polymers is limited by backbone flexibility and that the fraction of free volume is not the limiting factor for polymer mobility. The current study details our further efforts to understand the molecular relaxation processes of these new materials by analyzing the thermally stimulated depolarization currents (TSDC) spectrum in a wide temperature range.

The TSDC technique consists of measuring, with a defined heating and cooling scheme, the thermally stimulated discharge currents resulting from the release of the polarization that was frozen in during a previous electric field poling of the dielectric. TSDC analysis of polymers is a valuable tool for the study of the thermal relaxation properties of polymeric materials. Key advantages of this technique are its high

sensitivity, leading to the detection of very low dipole or carrier concentrations, and its very low equivalent frequency ( $\sim 1$  mHz), allowing multicomponent peaks to be resolved accurately. Generating better defined relaxation peaks that can be precisely analyzed helps in identifying molecular motions that cause different dielectric relaxations.

In this article, we present a model study, using the TSDC technique to investigate the dielectric relaxation mechanisms in a series of four homologous, tyrosine-derived polycarbonates with varying pendent chain lengths. These polymers contain four polar groups that can be expected to cause thermally stimulated depolarization currents. These groups are the carbonate and amide carbonyl in the polymer backbone and the ester carbonyl and methyl group located on the pendent chain (Fig. 1). In addition to the motion of these polar groups, the TSDC technique usually provides information about chain motions which occur at the glass transition. Our analysis of these relaxations was facilitated by the fact that the four test polymers differed only in the length of the alkyl ester pendent chain. Thus, observing the changes in the TSDC spectra as function of the pendent chain length helped in the identification of the molecular motions that caused specific relaxations and provided correlations with the structural properties of the polymers.

## EXPERIMENTAL

### Synthesis and Polymer Characterization

Tyrosine-derived polycarbonates were prepared according to previously published procedures.<sup>6,8</sup> The chemical structure of the polymers was confirmed by infrared and nuclear magnetic resonance spectroscopy. Molecular weights were determined by gel permeation chromatography (GPC) using a system consisting of a Perkin-Elmer Model 410 pump, a Waters Model 410 refractive index detector, and a Perkin-Elmer Model 2600 computerized data station. Two PL-gel GPC columns ( $10^5$  and  $10^3$  Å pore size, 30 cm in length) were operated in series at a flow rate of 1 mL/min in THF. Molecular weights were calculated relative to polystyrene standards without further corrections.

### Film Preparation

Polymeric films were cast on glass plates from a filtered (glass wool) 10% wt/vol solution in methylene chloride. The solvent was evaporated at room temperature under nitrogen. The films were then pressed for 10 min at 14,000 lb at a temperature of  $T_g + 40$  K between two heated, polished steel plates using a Carver Laboratory Press Model 2625. Before releasing the pressure, the plates were water-cooled to room temperature.

### TSDC Experiments

From the polymer films, round disc-shaped specimens (20 mm in diameter and 100 μm thick) were cut. These specimens were coated with evaporated aluminum on both surfaces to diminish the contact resistance between the electrodes and films. Coating also eliminated spurious currents due to electrostatic charges present at the sample surfaces. Each specimen was conditioned by heating above  $T_g$  followed by cooling at a rate of 55 K/min to the desired polarization temperature.

The TSDC experiments were performed from 77 to 400 K. A specimen was placed between two metallic terminal plates that were spring-loaded electrodes in electrical contact with the specimen's Al-coated surfaces. The TSDC measuring cell, after being evacuated to  $10^{-7}$  Torr, was filled with dry nitrogen at a pressure of 600 mmHg. The temperature was controlled by immersion of the cell in liquid nitrogen and by heating with a resistive element soldered to the external walls of

the cell. The polarizing dc field,  $E_p \cong 100$  kV/m, was applied for 3 min, long enough to orient the species under study. With the external field applied, the sample was then rapidly quenched (55 K/min) to 77 K. At this temperature, the field was switched off and the cell was evacuated for a second time and filled with dry helium (100 mmHg), which was used as an interchange gas due to its high purity and good thermal conductivity. A highly sensitive electrometer, Cary 401M, connected in series with the sample, detected the depolarization current density  $J_D$ , originating in the variations of the polarization  $P(T)$ , as the temperature was increased at a controlled, constant rate  $b$  (typically 6 K/min). The sensitivity of the system was  $10^{-17}$  A. The data acquisition system was fully automated. The analog output from the electrometer and the temperature were recorded concurrently by a voltmeter scanner and were stored in a PC computer for subsequent analysis.

### Analysis of TSDC Spectra

Direct signal analysis (DSA) is a curve-fitting procedure which was developed to analyze the complex TSDC peaks.<sup>9</sup> The method consists of finding the elementary curves whose characteristic energies are equally spaced in a given energy window and whose combination best fits the whole experimental TSDC profile. The recorded TSDC current is approximated by

$$J_D(T_j) = \sum_{i=1}^N \frac{P_{0i}}{\tau_i(T_j)} \exp \left[ -\frac{1}{b} \int_{T_0}^{T_j} \frac{dT'}{\tau_i(T')} \right], \quad (1)$$

$$(j = 1, m), (N \leq m)$$

where  $\tau(T)$  is the relaxation time for each elementary process,  $P_{0i}$  is its contribution to the total polarization, and  $b$  is the heating rate.

The temperature dependence of the relaxation time can be represented by either the Arrhenius [eq. (2)] or the Vogel-Fulcher [eq. (3)] expression, where  $T_0$  is the critical temperature at which the chain motions are frozen in the material:

$$\tau(T) = \tau_0 \exp \left( \frac{E}{kT} \right) \quad (2)$$

$$\tau(T) = \tau_0 \exp \left( \frac{E}{k(T - T_0)} \right) \quad (3)$$

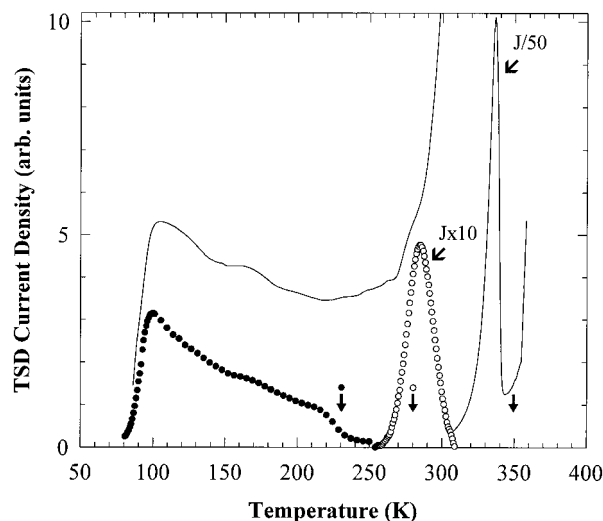


**Figure 2** Composite TSDC spectrum of poly(DTH carbonate) obtained from three separate experiments. The three polarization temperatures are indicated by arrows.

A nonlinear least-squares procedure was used where the initial parameters were the threshold and width of the energy window, the number of adjacent bins  $N$ , the  $N\tau_{oi}$ , and the starting values for  $P_{oi}$ , whose distribution was box-shaped, i.e., initially every bin contributed equally to the total polarization of the sample. The results of the fitting procedure were summarized in an energy histogram which covered the selected energy window divided into  $N$  energy bins and whose height,  $P_{oi}$ , was proportional to the area under the curve corresponding to each elementary excitation. The algorithm also fitted the  $\tau_{oi}$  values corresponding to each energy bin and the  $T_0$  value when the Vogel–Fulcher eq. (3) was used to present the relaxation times.

The DSA procedure was shown previously to work very well for  $\beta$  relaxations in poly(bisphenol-A carbonate),<sup>10</sup> as well as in the DGEBA–EDA epoxy resin system<sup>11</sup> and several other types of polymeric materials.<sup>12</sup> In all these cases, the temperature dependence of the relaxation times followed an Arrhenius law. A fit for the glass transition relaxation was performed for poly(bisphenol-A carbonate), but in this case, convergence was achieved only when Vogel–Fulcher relaxation times were used.<sup>9</sup> This temperature dependence was shown by many investigators to be adequate for transitions at  $T \geq T_g$ . A plausible basis for this dependence is provided by either the concept of free volume or by statistical thermodynamics.<sup>13</sup>

## RESULTS AND DISCUSSION

All the TSDC spectra reported in this work were normalized to the same polarizing field and sample area to make comparisons possible between the different samples studied. The TSDC spectra of the tyrosine-derived polycarbonates studied here consist of a broad band from 80 to 240 K, an intermediate zone which shows a peak at about 283 K, and a high-temperature region from 300 to 400 K, exhibiting a sharp peak that is the dielectric manifestation of the glass transition of the polymer. The glass transition peak is followed by a steep current increase due to the conductivity of the polymer. In Figure 2, the three regions of the TSDC spectrum of poly(DTH carbonate) are presented. This figure is the superposition of three different TSDC runs showing effectively the variety of relaxations present in the dielectric spectrum of this family of materials. The three polarization temperatures are indicated by arrows and the peak in the intermediate zone was partially “cleaned” in order to reduce the contribution of the low-temperature peaks.

The low-temperature TSDC spectra of the four polycarbonates are shown in greater detail in Figure 3. The current density has been normalized to the same polarizing field and sample size. It is readily seen that the  $\beta$  relaxation is a complex band resulting from the superposition of several molecular processes whose absolute and relative contributions to the total polarization vary with

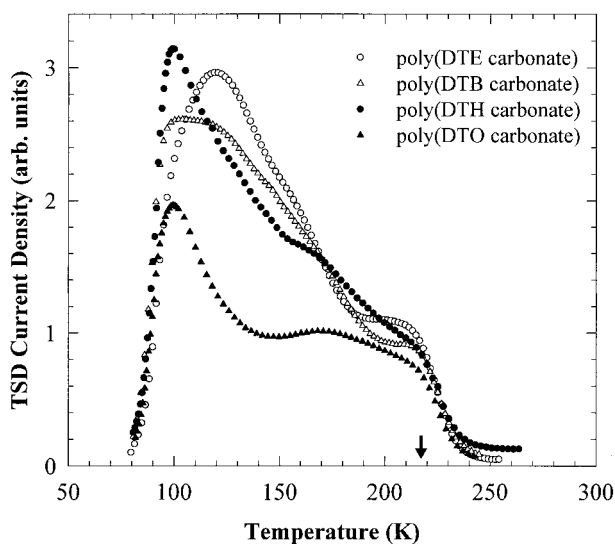


**Figure 3** Low-temperature TSDC spectra for poly(DTE carbonate), poly(DTB carbonate), poly(DTH carbonate), and poly(DTO carbonate).

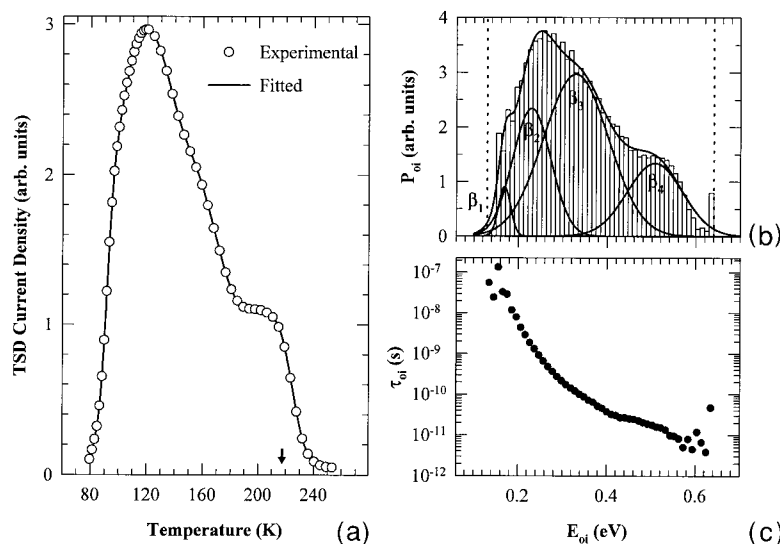


**Figure 4** DSA analysis of the  $\beta$  peak in poly(DTE carbonate): (a) experimental and fitted peak; (b) energy histogram of the contribution to the polarization of each energy bin; (c) variation of the Arrhenius preexponential factor with the activation energy.

the length of the pendent chain. The complexity of the recorded trace demands a sophisticated analysis if quantitative information is to be extracted from these data.

To study the different relaxation processes that cause the broad  $\beta$ -peak, the direct signal analysis (DSA) method was applied to the whole low-temperature TSDC spectrum. Representative results of the DSA method are shown in Figure 4 for poly(DTE carbonate). For the curve fitting [Fig. 4(a)], Arrhenius relaxation times were assumed in the analysis of these low-temperature relaxations which are due to localized motions of molecular segments of variable lengths. The energy window for the best fit ranged from 0.1 to 0.7 eV and the resulting energy histogram is shown in Figure 4(b). The variation of the preexponential factor  $\tau_{0i}$  corresponding to each energy bin is plotted in Figure 4(c). The energy histogram was fitted to four components, assuming a Gaussian profile for each of them. The four Gaussian curves were labeled in the order of increasing energy ( $\beta_1$ ,  $\beta_2$ ,  $\beta_3$ ,  $\beta_4$ ). All four polycarbonates tested had these four components in their respective energy histograms. A careful examination of the experimental trace also reveals the existence of four reorientation processes, and by choosing carefully the experimental conditions and by applying "cleaning" techniques, the same four peaks could be isolated. The problem with such a procedure, however, is that the energy distribution of the isolated peaks is altered by the peak "cleaning"

procedure, whereas if the complex peak is analyzed, the sought distribution is not perturbed.

The mean reorientation energy and the relative intensities of these peaks varied with  $n$  (the pendent chain length) in different ways. In Table I, the characteristic parameters (mean energy and width values) for the four Gaussian distributions are presented. The mean energies of the  $\beta_1$  and  $\beta_2$  components remain constant, around 0.17 and 0.23 eV, respectively, as the length of the pendent chain changes. However, for the  $\beta_3$  and  $\beta_4$  components, the mean energies decrease slightly up to  $n = 6$  and increase for  $n = 8$ . Next, the relative intensities of the four  $\beta$  peaks were plotted as a function of  $n$  (Fig. 5). The dependence on  $n$  of the relative intensity of the  $\beta_i$  components was different for each of the four peaks. The relative intensity of the  $\beta_1$  peak increases slightly with  $n$ , the relative intensity of the  $\beta_2$  peak is approximately independent of  $n$ , the relative intensity of the  $\beta_3$  shows a maximum at  $n = 6$ , while the relative intensity of the  $\beta_4$  peak has a minimum at  $n = 6$ .

The absolute values of the polarization originated by each  $\beta_i$  component, as well as the total polarization of the whole complex  $\beta$  band as a function of  $n$ , are calculated from the respective areas under the curves and are shown in Figure 6. The calculation was done for an electric field strength of 1 V/ $\mu\text{m}$ . The straight line in Figure 6 represents the expected decay of the total polarization following the decrease in the measured

**Table I** Mean Energy and Width for the Gaussian Profiles of the Components of the  $\beta$ -Relaxation

$n$	$E_{0\beta_1}$ ( $\sigma_{\beta_1}$ ) (eV)	$E_{0\beta_2}$ ( $\sigma_{\beta_2}$ ) (eV)	$E_{0\beta_3}$ ( $\sigma_{\beta_3}$ ) (eV)	$E_{0\beta_4}$ ( $\sigma_{\beta_4}$ ) (eV)	Density (g/cm <sup>3</sup> )
2	0.17 (0.03)	0.23 (0.10)	0.33 (0.17)	0.51 (0.15)	1.25
4	0.17 (0.04)	0.22 (0.09)	0.31 (0.17)	0.49 (0.30)	1.22
6	0.18 (0.04)	0.23 (0.08)	0.31 (0.16)	0.46 (0.30)	1.19
8	0.18 (0.05)	0.23 (0.09)	0.35 (0.18)	0.51 (0.17)	1.16

density reported in Table I. This estimate was done starting from the total polarization measured for  $n = 2$  and multiplying this value by a factor  $p_{n>2}/p_2$  for  $n = 4, 6, 8$ . The variation of the total polarization (represented by the filled symbols in Fig. 6) follows the expected decay closely up to  $n = 6$ .

The above observations make it possible to identify the molecular relaxations associated with each of the four  $\beta$  components. The origin of the dielectric  $\beta$  relaxations in poly(bisphenol-A carbonate) has been attributed to the local motions of small polar groups,<sup>14</sup> e.g., the motion of methyl and carbonate groups. Our results relating to the  $\beta$  relaxations of tyrosine-derived polycarbonates appear to confirm this assumption. The  $\beta_1$  peak should originate from the most easily reorientable dipoles for they have the lowest reorientation energy. Likewise, they should also have the smallest dipole moment as they produce the smallest contribution to the total polarization. Consequently,

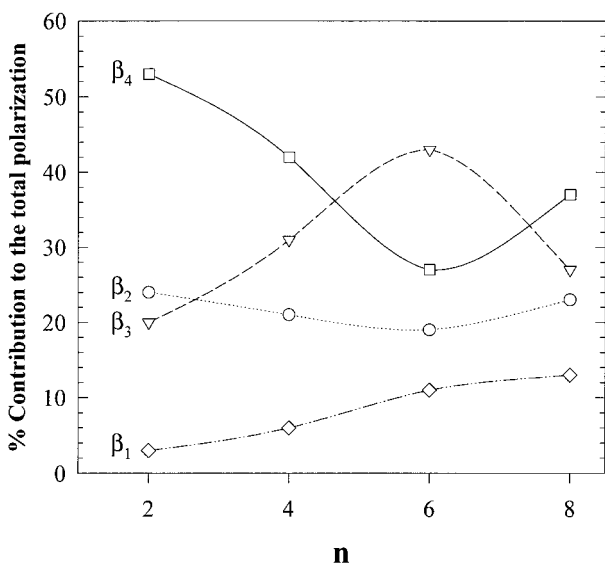


**Figure 5** Variation of the percentage for each contribution to the total polarization for the  $\beta_i$  peaks as a function of  $n$ . The lines are drawn to guide the eye.

the  $\beta_1$  peak can be assigned to the orientable dipoles of the CH<sub>3</sub> end groups of the pendent chain. The increasing effective number of reorientable CH<sub>3</sub> dipoles with increasing  $n$  can be explained by the associated decrease in packing efficiency reported previously.<sup>6</sup> Furthermore, nuclear magnetic resonance analysis of poly(bisphenol-A carbonate)<sup>15</sup> revealed that the protons of methyl groups undergo a motional narrowing of line width in the temperature region from 110 to 130 K. This is the temperature range of the  $\beta_1$  peak observed here. In addition, the activation energy of the relaxation process for methyl groups in poly(bisphenol-A carbonate) has been reported<sup>16</sup> to be about 0.2 eV based on ultrasonic attenuation experiments at 10 MHz. This is very close to the values obtained here from the analysis of the  $\beta_1$  component (see Table I).

The relative contribution of the  $\beta_2$  component to the total polarization is nearly independent of

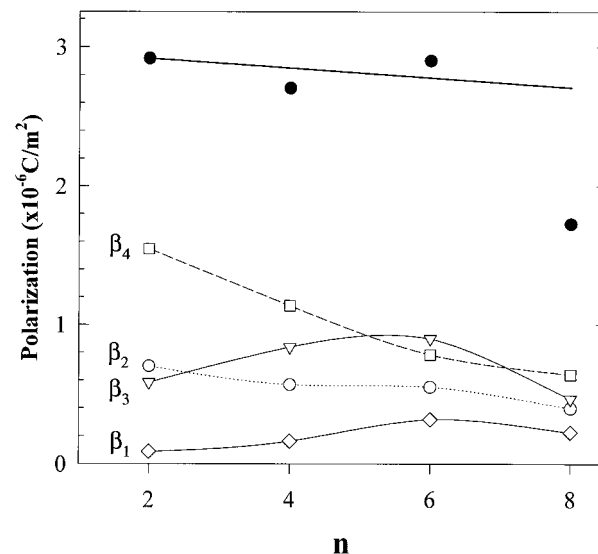


**Figure 6** Variation of the absolute values of the polarization originated by each  $\beta_i$  component as well as the total polarization of the whole complex  $\beta$  band ( $\bullet$ ) as a function of  $n$ . The lines are drawn to guide the eye.

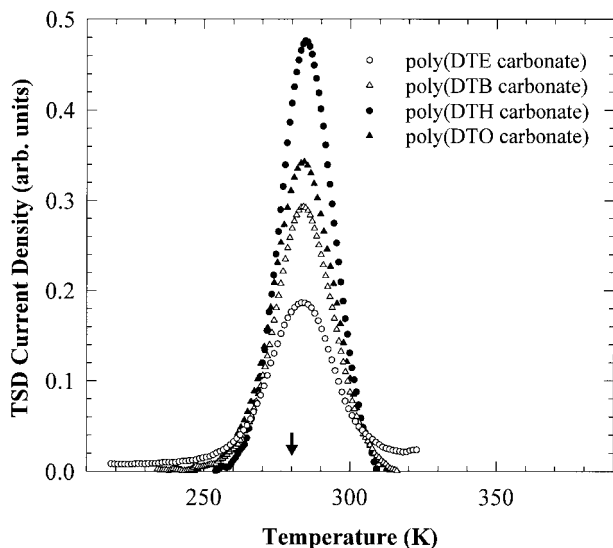


**Figure 7** Intermediate-temperature TSDC spectra for poly(DTE carbonate), poly(DTB carbonate), poly(DTH carbonate), and poly(DTO carbonate). The peaks were partially “cleaned” on the low-temperature side.

$n$  (Fig. 6), indicating that the number of reorientable species is not sensitive to the length of the pendent chain. Since the carbonate–carbonyl segments close to the phenyl rings are the dipolar units farthest from the pendent chain, the  $\beta_2$  component is assumed to be associated with the motion of the carbonate carbonyl group. The activation energies obtained for this process are 0.23 eV (Table I) and agree well with the reported values<sup>17</sup> of the relaxations associated with movements of the carbonate groups in poly(bisphenol-A carbonate).

The  $\beta_3$  component is assigned to the motion of the ester-bonded carbonyl groups. This assignment is supported by the following observations: The decrease in the polymer’s packing efficiency with  $n$  can account for the initial increase in the contribution to the polarization of the  $\beta_3$  peak (see Fig. 5). However, the decrease in the relative intensity of this contribution for  $n = 8$ , together with an increase in the reorientation energy, points to a reorientation process that is affected by the degree of entanglement of the pendent chains which is most pronounced for  $n = 8$ . Thus, the  $\beta_3$  component should originate from the motion of dipoles located on the pendent chain.

The partial double-bond character of the C—N bond leads to a rigid, planar configuration for the amide carbonyl located on the polymer main chain. Due to its rigid environment, the relaxation

of this dipole should have the highest mean activation energy. Thus, the  $\beta_4$  peak is tentatively assigned to the motion of the amide carbonyl. This hypothesis is supported by the initial decrease with  $n$  of the relative contribution of the  $\beta_4$  component: It seems that the  $\beta_4$  contribution originates at a carbonyl group whose motion is hindered by the increasing length of the pendent chain. The sudden enhancement of the  $\beta_4$  component for  $n = 8$  (shown in Fig. 5) can be explained considering that pendent chain entanglements at  $n = 8$  reduce the effectiveness of the pendent chain in suppressing the motion of the structural elements located in the polymer backbone.

The isolated intermediate relaxations shown in Figure 7 were obtained by applying the same polarizing conditions to all the samples studied here. Furthermore, to make valid comparisons between the different polymers, the data were normalized to the same sample dimensions and similar “cleaning procedures” were used in all calculations. The DSA with Arrhenius dependencies for  $\tau(T)$  was used to obtain the characteristic parameters for these relaxations. On their high-temperature side, the obtained energy histograms were perturbed by the tail of the strong glass transition peak. A single Gaussian profile fitted the energy histogram for each of the polymers. The mean energy and width of the Gaussian distribution are presented in Table II as a function of  $n$ . The continuous growth of this band’s height reaching a maximum for  $n = 6$  indicates that the dipoles involved in this process could be located on the pendent chains, whose increasing length decreases the packing efficiency, and, therefore, favors the number of reorienting segments. The decrease of the band intensity for  $n = 8$  can be explained by assuming that pendent chain entanglement effects are no longer negligible in the polymer having the longest pendent chain. The high mean activation energies reported here are associated with low preexponential Arrhenius factors which could be due to the overlapping of the  $\alpha$  transition

**Table II** Mean Energy and Width for the Gaussian Profile of the Intermediate Relaxation

$n$	$E_0$ (eV)	$\sigma$ (eV)
2	1.60	0.26
4	1.68	0.35
6	1.73	0.30
8	1.73	0.28

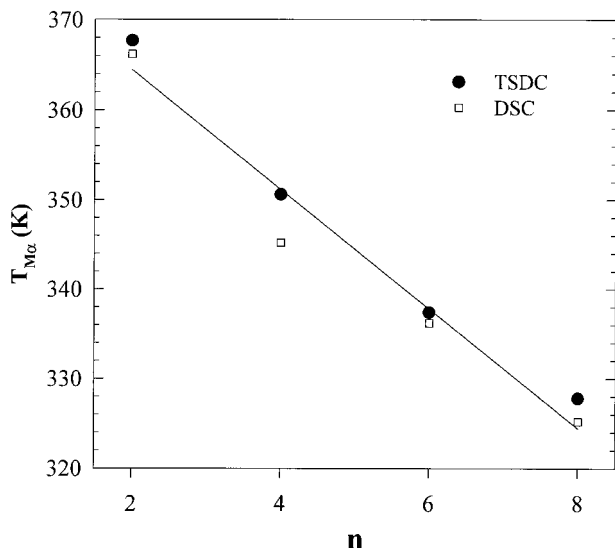


**Figure 8** Variation of the temperature of the maximum of the TSDC  $\alpha$ -peaks along with the glass transition temperatures obtained from previous DSC experiments,<sup>6</sup> as a function of  $n$ .

whose intensity and position differs with  $n$ . These values may be interpreted as being indicative of the involvement of larger molecular structures in the reorientation process and it is possible that the intermediate temperature relaxation is the result of the reorientation of the entire pendent chain whose motion would be the precursor movement of the primary glass transition. This interpretation could also explain the energy shift, reported in Table II, to higher values as  $n$  increases since longer pendent chains should require higher energies to participate in the relaxation process. This interpretation of the experimental data is appropriate since the tested polymers are fully amorphous, eliminating the need to consider the intermediate peak which is usually observed in semicrystalline polymers. However, our results do not exclude smaller molecular segments in deeper potential wells as the responsible relaxing entity.

The high-temperature zone of the TSDC spectrum (Fig. 2) shows a very intense and sharp event, the  $\alpha$ -peak, indicative of the glass transition relaxation, followed by a steep increase in the recorded current. The temperature of the current maximum for this peak,  $T_{M\alpha}$ , decreased as the pendent chain length increased (Fig. 8). The TSDC values obtained for the temperature of the maximum of the four peaks along with the glass transition temperatures obtained from previous DSC experiments<sup>6</sup> are plotted as a function of  $n$  in Figure 8. A good correlation between the TSDC

and DSC measurements, performed with similar heating rates, was observed. The DSA of these peaks converged only when Vogel–Fulcher dependencies for the relaxation times were considered. The need for a Vogel–Fulcher model in the analysis of the glass transition peak confirms previous results for poly(bisphenol-A carbonate).<sup>9</sup>

The results obtained with DSA analysis of the glass transition of poly(DTH carbonate) are presented in Figure 9. The energy histogram clearly shows a nearly monoenergetic process which is a common characteristic observed in the  $\alpha$ -transition of all the polymers studied here. Using the characteristic parameters obtained from DSA, the fractional free-volume expansion coefficient  $\alpha_f$  at  $T = T_{M\alpha}$  can be estimated from the inverse of the Vogel–Fulcher energy ( $k/E = \alpha_f$ ). The resulting fractional free volumes are presented in Table III. The fitted  $T_0$  values are a decreasing function of  $n$ , in accordance to the observed experimental dependence of  $T_{M\alpha}$ . The values of  $T_{M\alpha} - T_0 = (65 \pm 5)$  K and  $T_{M\alpha}/T_0 = (1.23 \pm 0.02)$  are constant within 6 and 2%, respectively. This is in agreement with the Adam and Gibbs theory.<sup>13</sup>

The increase of the calculated fractional free volumes and the decrease of the measured densities with increasing pendent chain length (see Table I) are in good agreement with the changes in flexibility previously reported for these polymers.<sup>6</sup> The values for the calculated fractional free volume at  $T = T_{M\alpha}$  (Table III) are reasonable for polymers having branches consisting of alkyl chains of increasing length.

## CONCLUSIONS

The detailed analysis of the TSDC spectra obtained from a homologous series of four tyrosine-derived polycarbonates with different pendent chains has allowed the identification of several relaxation mechanisms. Assignment of some of the TSDC peaks to the motion of specific molecular structures was facilitated by interpreting the changes in the TSDC spectra as function of the pendent chain length  $n$ . For the low-temperature, multicomponent  $\beta$  relaxation, the observed strength, activation energy, and preexponential factor variations of the different  $\beta_i$  components is consistent with motions of small polar entities with increasing reorienting energies. As the length of the pendent chain ( $n$ ) is increased, the four  $\beta$  relaxations are affected differently. The mean energies of the  $\beta_2$  component are not depen-



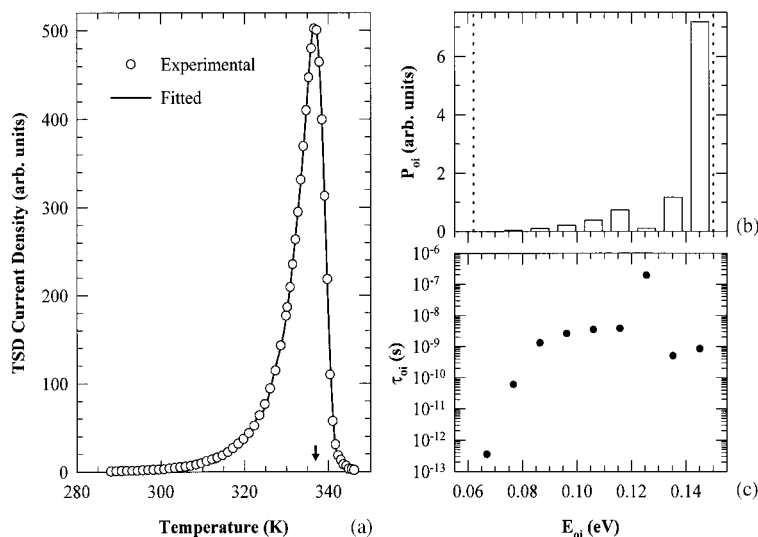


**Figure 9** DSA analysis of the  $\alpha$ -peak in poly(DTH carbonate): (a) experimental and fitted peak; (b) energy histogram of the contribution to the polarization of each energy bin; (c) variation of the Arrhenius preexponential factor with the activation energy.

dent on  $n$  and the relative contributions of the  $\beta_1$  and  $\beta_2$  components to the total polarization vary only slightly while  $\beta_1$ 's contribution is always less than 13%. On the other hand, the relative contributions of the  $\beta_3$  and  $\beta_4$  components to the total polarization vary significantly as the pendent chain increases in length. The  $\beta_3$  and  $\beta_4$  components are also affected by pendent chain entanglement. Thus, the  $\beta_1$  peak is assigned to the motion of the  $\text{CH}_3$  group found in all pendent chains. The  $\beta_2$  peak is assigned to the motion of the carbonate carbonyl group present in the polymer backbone. The  $\beta_3$  peak is assigned to the motion of the ester carbonyl present in the pendent chain. The  $\beta_4$  peak may be associated with the motion of the amide carbonyl in the polymer backbone. This assignment was made considering the chemical structure of the polymer (Fig. 1) and the known rigidity of the amide carbonyl group.

The high activation energies associated with the intermediate temperature transition (283 K) may be interpreted as being caused by a relatively

large reorienting entity. The variation in the intermediate transition as a function of the pendent chain length shows that chain entanglement effects are predominant for  $n = 8$ . These observations indicate that the observed TSDC peak is caused by the mobility of the entire pendent chain as a precursor to the backbone motion occurring at  $T_g$ .

The dielectric manifestation of the glass transition is the  $\alpha$  peak which is an almost monoenergetic Vogel–Fulcher relaxation. The position of this peak is in correspondence with the glass transition temperatures measured for these polymers by differential scanning calorimetry. The variation in the calculated fractional free volume and  $T_0$  values derived from DSA as function of  $n$  are consistent with the increase in flexibility observed for polymers with longer pendent chains.<sup>6,7</sup>

Financial support from the Consejo Nacional de Investigaciones Científicas y Tecnológicas (CONICIT), Caracas, Venezuela, is gratefully acknowledged by N. S.,

**Table III** Glass Transition Peak: Variation of DSA Results with  $n$

$n$	$E$ (eV)	$T_0$ (K)	$\tau_0$ (s)	Fractional Free Volume (at $T = T_{M\alpha}$ )
2	0.145	300.8	$3.3 \times 10^{-10}$	3.9%
4	0.118	290.2	$4.7 \times 10^{-9}$	4.4%
6	0.145	267.3	$8.5 \times 10^{-10}$	4.1%
8	0.097	264.7	$6.4 \times 10^{-10}$	5.6%

E. L., and A. B. This work is part of Project NM-012 of the Programa de Nuevas Tecnologías. The work at Rutgers University was supported by NIH Grant GM39455. The authors thank Mr. Tangpasuthadol for preparation of the polymer samples and acknowledge the editorial assistance of Ms. Carole Kantor.

## REFERENCES

1. D. Coffey, Z. Dong, R. Goodman, A. Israni, J. Kohn, and K. O. Schwarz, in *Symposium on Polymer Delivery Systems*, presented at the 203rd Meeting of the American Chemical Society, San Francisco, CA, 1992, p. CELL 0058.
2. Z. Dong, MSc Thesis, Rutgers University, 1993.
3. S. I. Ertel, J. Kohn, M. C. Zimmerman, and J. R. Parsons, *J. Biomed. Mater. Res.*, **29**(11), 1337 (1995).
4. J. Choueka, J. L. Charvet, K. J. Koval, H. Alexander, K. S. James, K. A. Hooper, and J. Kohn, *J. Biomed. Mater. Res.*, **31**, 35 (1996).
5. J. Kohn, *Trends Polym. Sci.*, **1**(7), 206 (1993).
6. S. I. Ertel and J. Kohn, *J. Biomed. Mater. Res.*, **28**, 919 (1994).
7. V. Tangpasuthadol, A. Shefer, K. A. Hooper, and J. Kohn, *Biomaterials*, **17**(4), 465 (1996).
8. S. Pulapura and J. Kohn, *Biopolymers*, **32**, 411 (1992).
9. M. Aldana, E. Laredo, A. Bello, and N. Suarez, *J. Polym. Sci. Part B Polym. Phys.*, **32**(13), 2197 (1994).
10. E. Laredo, M. Aldana, J. Müller, A. Bello, and N. Suarez, in *Annual Report of the IEEE Conference on Electric Insulation and Dielectric Phenomena*, 1995, p. 432.
11. E. Laredo, M. Aldana, N. Suarez, A. Bello, and M. Diaz, *Mater. Eng.*, **4**(2), 237 (1993).
12. E. Laredo, N. Suarez, A. Bello, and L. Marquez, *J. Polym. Sci. Polym. Phys. Ed.*, **34**, 641 (1996).
13. G. Adam and J. H. Gibbs, *J. Chem. Phys.*, **43**(1), 139 (1965).
14. Y. Aoki and J. O. Brittain, *J. Appl. Polym. Sci.*, **20**(10), 2879 (1976).
15. S. Matsuoka and Y. Ishida, *J. Polym. Sci. Part C*, **14**, 247 (1966).
16. Y. Tanabe, J. Hirose, K. Okano and Y. Wada, *Polym. J.*, **1**(1), 107 (1970).
17. B. B. Sauer and P. Avakian, *Polymer*, **33**(24), 5128 (1992).